




## Original Article

# An Improved Electron Microprobe Method for the Analysis of Halogens in Natural Silicate Glasses

Stamatis Flemetakis<sup>1\*</sup> , Jasper Berndt<sup>1</sup>, Stephan Klemme<sup>1</sup>, Felix Genske<sup>1</sup> , Anita Cadoux<sup>2</sup> , Marion Louvel<sup>1</sup> and Arno Rohrbach<sup>1</sup>

<sup>1</sup>Institut für Mineralogie, Westfälische Wilhelms-Universität Münster, Corrensstraße 24, 48189 Münster, Germany and <sup>2</sup>Cogitamus Laboratory, Saint-Aubin, Île-de-France, France

## Abstract

We present a new analytical method, which allows the simultaneous analysis of fluorine (F), chlorine (Cl), bromine (Br), and iodine (I) in geological samples. To account for interferences of Fe on the spectral lines of F, of Al on Br-lines, and of Ca on I-lines, we prepared four new halogen-free calibration glasses. The new method is used to analyze various glass reference materials and crystal-hosted melt inclusions from the Azores. Our results show that our new method allows reliable and reproducible analyses of all four halogens in silicate glasses.

**Key words:** bromine, electron probe microanalysis, fluorine, halogens, iodine

(Received 14 April 2020; revised 24 June 2020; accepted 17 July 2020)

## Introduction

The halogens, fluorine (F), chlorine (Cl), bromine (Br) and iodine (I), exert an important role in many magmatic and hydrothermal processes (Harlov & Aranovich, 2018). Nevertheless, their geochemical behavior in most geological settings is not well understood, mostly due to a lack of reliable geochemical analyses (see Klemme & Stalder (2018) for some discussion). Halogens can be analyzed in geological samples using various analytical techniques, including secondary ion mass spectrometry (SIMS) (e.g., Hinton, 1990; Straub & Layne, 2003; Kusebauch et al., 2015; Cadoux et al., 2017), noble gas mass spectrometry (e.g., Kendrick et al., 2012), instrumental neutron activation (INAA) (e.g., Marks et al., 2012; Cadoux et al., 2017), microbeam X-ray fluorescence ( $\mu$ -XRF) spectrometry (e.g., Pan & Dong, 2003), laser ablation inductively coupled mass spectrometry (LA-ICP-MS) (e.g., Hammerli et al., 2013) and electron probe microanalysis (EPMA) (e.g., Zhang et al., 2016, 2017). Compared with most of the methods mentioned above, advantages of EPMA are (a) the availability in most geoscience institutes, (b) excellent spatial resolution, (c) relatively low analytical costs, and (d) simultaneous determination of all four halogens. Until recently though, halogen analyses with EPMA were hindered by relatively high detection limits (DLs), e.g., 600–1,200  $\mu\text{g/g}$  for F, due to low count rates when using thallium

acid phthalate (TAP) crystals (Potts & Tindle, 1989), or spectral interferences when using multilayered crystals (Potts & Tindle, 1989).

The main problems associated with EPMA of halogens are: (1) spectral interferences between Fe on F, Al on Br, and Ca on I in rock-forming minerals and glasses and (2) lack of well-characterized EPMA reference materials that cover the broad range of halogen concentrations in natural minerals and glasses as well as (3) lack of low Al and low Ca EPMA calibration materials to estimate correction factors for Br and I analyses.

As to spectral interferences, EPMA of reference materials like the Kakanui Hornblende (USNM 143965) (Jarosewich et al., 1980) and the Durango fluorapatite (Marks et al., 2012) revealed that the first-order  $\text{FeL}_{\alpha}$  and  $\text{FeL}_{\beta}$ , and the second-order  $\text{MgK}_{\alpha}$  and  $\text{MgK}_{\beta}$  spectral lines interfere with the  $\text{FK}_{\alpha}$  line. Marks et al. (2012) showed that the  $\text{FeL}_{\alpha}$  line overlaps at the peak position of the  $\text{FK}_{\alpha}$ , while the  $\text{MgK}_{\beta}$  line overlaps at the right-side background position of the  $\text{FK}_{\alpha}$ . Bromine analyses are affected by interferences from Al-lines, e.g., as  $\text{ALK}_{\alpha}$  and  $\text{ALK}_{\beta}$  interfere with the adjacent  $\text{BrL}_{\alpha}$  and  $\text{BrL}_{\beta}$  lines (Fleet, 1989; Zhang et al., 2017). Finally, spectral interferences for  $\text{IL}_{\alpha}$  result from the  $\text{K}_{\beta}$  line of Ca.

Zhang et al. (2016, 2017) developed specific analytical protocols for EPMA analysis of F and Br in geological samples. Analysis of F with a TAP crystal is possible as there is no spectral interference, but obtained count rates are usually too low for meaningful analysis (Zhang et al., 2016), unless more than one TAP crystals are used (Bénard et al., 2017). Instead, F is preferentially measured using a W-Si-multilayered pseudocrystal as the diffraction crystal (Zhang et al., 2016). This is the method of choice, as higher count rates result in lower DLs (82–106  $\mu\text{g/g}$

\*Author for correspondence: Stamatis Flemetakis, E-mail: [stam.flemetakis@uni-muenster.de](mailto:stam.flemetakis@uni-muenster.de)

Cite this article: Flemetakis S, Berndt J, Klemme S, Genske F, Cadoux A, Louvel M, Rohrbach A (2020) An Improved Electron Microprobe Method for the Analysis of Halogens in Natural Silicate Glasses. *Microsc Microanal* 26, 857–866. doi:10.1017/S1431927620013495

for F). As to the overlap on  $FK_{\alpha}$  from the second-order  $MgK_{\beta}$  line, Zhang et al. (2016) used the EPMA in a differential mode with an optimized PHA (pulse height analysis) setting in signal processing, which completely eliminated interferences from the second-order  $MgK_{\beta}$  line. The overlapping first-order  $FeL_{\alpha}$  on  $FK_{\alpha}$  peak cannot be filtered by modifying the PHA settings and was instead calibrated quantitatively using a few F-free, Fe-bearing natural silicate glasses and minerals. Using this approach, Zhang et al. (2016) demonstrate the successful analysis of F in a number of reference glasses (VG-2, VG-A99, VG-568, and BCR-2G), as well as in synthetic glasses made from powders of some rock reference materials (AC-E, GS-N, and DR-N).

For the EPMA analysis of Br, Zhang et al. (2017) established an analytical protocol by using Br-free but Al-bearing materials to quantify the overlap from  $AlK_{\alpha}$  on  $BrL_{\beta}$  lines. The count rate of the  $BrL_{\beta}$  peak signal was enhanced by high beam currents (100–200 nA) and long measurement times (120 s at the peak position and 60 s at the background). The application of this protocol to Al- and Br-bearing materials, such as sodalite and scapolite, and to five synthetic glasses yielded Br concentrations in the range of 250–4,000  $\mu\text{g/g}$  that were consistent with those measured by microbeam synchrotron X-ray fluorescence ( $\mu$ -SXRF) spectrometry (Zhang et al., 2017). The EPMA method presented by Zhang et al. (2017) has a Br detection limit of  $\sim 100$ – $300 \mu\text{g/g}$ .

To our knowledge, no such EPMA protocol has been established for I analyses in natural and experimental silicate glasses. Iodine analyses are more complicated, as I concentrations in natural glasses are extremely low (i.e., tens to hundreds ng/g, Kendrick, 2012; Kendrick et al., 2013; 2015), and EMPA detection limits ( $\sim 150 \mu\text{g/g}$ ; e.g., Lerouge et al., 2010) are higher than those for F and Br. The EPMA analysis of Cl in geological samples requires no special treatment.

The second problem with halogen analysis of geological samples with the EPMA is due to the fact that well-characterized halogen-bearing reference materials are scarce. Recently, Cadoux et al. (2017) produced Br-bearing silicate glasses with concentrations from 0.5 to 6,000  $\mu\text{g/g}$ . Attempts to calibrate EPMA standards for Br in basaltic (with  $\sim 6,000$  ppm Br; Cadoux et al., 2017) and haplogranite glass (with  $0.96 \pm 0.04$  wt% Br, Louvel et al., 2020) have also been recently reported. Zhang et al. (2016) synthesized F-bearing glasses in granitic and dioritic rock compositions, which have been used as reference materials for bulk halogen analyses. However, to our knowledge, no I-bearing reference material glasses are available.

In principle, halogens can be determined using various analytical techniques, e.g., SIMS (e.g., Straub & Layne, 2003; Kusebauch et al., 2015; Cadoux et al., 2017), noble gas method (e.g., Kendrick et al., 2012), INAA (e.g., Marks et al., 2012; Cadoux et al., 2017),  $\mu$ -XRF spectrometry (e.g., Pang & Dong, 2003), EPMA (e.g., Zhang et al., 2016, 2017), and others. Compared with most of the methods mentioned above, EPMA advantages are (a) the ease of access in such instruments, (b) reasonable spatial resolution ( $< 1 \mu\text{m}$ ), (c) relatively low analytical costs, and (d) simultaneous determination of all four halogens. Until recently though, halogen analyses with EPMA were hindered by relatively high DLs (600–1,200  $\mu\text{g/g}$  for F, while Br data are rare) and low count rates when using TAP crystals (Potts & Tindle, 1989), and spectral interferences when using multilayered crystals (Potts & Tindle, 1989). The analytical protocols by Zhang et al. (2016, 2017) tackled the problem generated by spectral interferences in F and Br analyses, hence leading to higher count rates and lower DLs (106  $\mu\text{g/g}$  for F and between 120 and 300  $\mu\text{g/g}$

for Br). Still, these DLs, especially for Br and I, are too high for obtaining reasonable analyses in natural samples (although, in some case, Br concentrations can reach up to 300  $\mu\text{g/g}$  in melt inclusions and matrix glasses; Bureau & Métrich, 2003). But they can be particularly useful in experimental petrology in order to determine partition coefficients for these elements, especially I, in magmatic and/or hydrothermal systems, thus evaluating the behavior of these elements in such systems. However, further improvement of these analytical protocols is required, particularly an assessment of the methods at lower F and Br contents, improved DLs, and establishment of an analytical protocol for I analyses in geological materials.

## Rationale

To improve the analytical EPMA techniques for the analysis of halogens in natural samples, we set out to prepare an improved analytical protocol. To achieve this, we prepared new synthetic halogen-free glasses in different compositions to improve the calibration of interferences during halogen analysis with EPMA, and we also present a new analytical protocol for I analyses in silicate glasses. Furthermore, we synthesized two halogen-bearing silicate glasses to examine the accuracy of our calibration for F, Br, and I. Fluorine and Br analyses of silicate glasses were conducted using the analytical protocols of Zhang et al. (2016, 2017), and I using our own new analytical protocol. These new reference materials and improved EPMA methods can be applied to geological investigations that require high spatial resolution, e.g., experimental studies (e.g., Steenstra et al., 2020), or the study of melt inclusions (e.g., Métrich et al., 2014; Rose-Koga et al., 2017; present study).

## Materials and Methods

The EPMA methods of Zhang et al. (2016, 2017) rely on a set of halogen-free reference materials to calibrate spectral interferences during EPMA measurements. In our laboratory, we use similar glasses (see below) but we also synthesized several new halogen-free glasses (Table 1) to improve the calibration of interferences during halogen analysis, and we also analyzed various halogen-bearing glasses, including well-known reference materials and newly synthesized glasses (Tables 2–5). All synthesis experiments were performed in the experimental petrology laboratory of the Institute for Mineralogy at the University of Münster, Germany. The halogen-free glasses are of basaltic, rhyolitic, and enstatitic composition and were synthesized using analytical grade oxides and salts in a piston-cylinder apparatus at high pressures and high temperatures ( $P = 1$  GPa,  $T = 1,450^{\circ}\text{C}$ , 36 h run duration), or in gas-mixing furnaces at atmospheric pressure (Table 1). Samples were loaded into Pt-capsules. The halogen-bearing glasses include all halogens (F, Cl, Br, and I) and their halogen concentrations are 1,000 and 5,000  $\mu\text{g/g}$  for each (Table 5). Backscattered electron images of the resulting glasses showed that the samples were completely quenched, and EPMA analyses showed only small compositional heterogeneity (small errors, Tables 2–4).

The new halogen-free glasses were used to quantify the Fe, Al, and Ca interferences on F, Br, and I peaks, and this allowed us to construct calibration lines (Figs. 1a–1c) that can be used to subtract the amount of “apparent” halogen (Table 1), arising from the interfering Fe, Mg, Al, or Ca. To evaluate the accuracy of our method, we analyzed several independent reference material glasses available in the literature (Tables 2–4).

**Table 1.** Major Elements (wt%) Composition and “Apparent” Halogen Contents ( $\mu\text{g/g}$ ) of Halogen-Free Glasses Used for the Calibration.

Glass	FeO	SD	“F”	SD	Al <sub>2</sub> O <sub>3</sub>	SD	“Br”	SD	CaO	SD	“I”	SD
CB (VdK) <sup>1</sup>	1.1	0.1	350	52	16	0.3	798	39	5.7	0.1	279	20
Mercury surface <sup>2</sup>	1.8	0.1	370	45	14	0.2	710	20	6.0	0.1	282	16
NP-LMg (VdK) <sup>1</sup>	1.6	0.1	387	51	12	0.2	578	31	5.4	0.1	260	14
Mars regolith <sup>2</sup>	0.09	0.06	262	50	13	0.2	657	76	6.8	0.2	316	21
Mars surface <sup>2</sup>	13	0.3	1152	158	11	0.2	548	24	5.7	0.2	280	19
B1 <sup>3</sup>	8.6	0.3	805	100	16	0.2	755	40	12	0.2	564	19
B2 <sup>3</sup>	10.5	0.11	909	96	16	0.2	727	35	10	0.3	489	13
S1-low Ca(GI-2) <sup>4</sup>	n.a.	n.a.	n.a.	–	14	0.4	687	25	1.15	0.15	75	14
S2-low Al(GI-1) <sup>4</sup>	n.a.	n.a.	n.a.	–	1.4	0.1	83	25	9	0.3	448	38
S3-high Ca(GI-3) <sup>3</sup>	n.a.	n.a.	n.a.	–	16	0.4	759	14	14	0.5	624	21
S4-high Al (GI-4) <sup>3</sup>	n.a.	n.a.	n.a.	–	17	0.4	845	9	n.a.	n.a.	24	10

Synthetic halogen-free glasses are used to establish the calibration lines. “F”, “Br”, and “I” refer to “apparent” halogen contents that are caused by the interferences of Fe on F-line, Al on Br-line, and Ca on I-line. The glasses were prepared by: <sup>1</sup>Morlok et al. (2017), <sup>2</sup>Morlok et al. (2019), <sup>3</sup>Berndt et al. (2005), and <sup>4</sup>present study. Refer to these studies for detailed information.

**Table 2.** Reference Glasses Analyzed in the Present Study and Their F, Cl contents ( $\mu\text{g/g}$ ).

Glass	F	Error	Error%	Cl	Error	Error%
VG-2 (Juan de Fuca)	197	46	23	275	18	6.5
VG-A99 (Makaopuhi)	585	26	4.4	210	7	3.3
VG-568 (Rhyolite)	1,794	21	1.2	1,015	24	2.4
BCR-2G	167	19	11	38	9	24
AC-E <sup>1</sup>	1,885	20	1.1	303	7	2.3
GS-N <sup>1</sup>	963	22	2.3	472	4	0.8
DR-N <sup>1</sup>	586	20	3.4	475	3	0.6
NMNH 113716/11	153	41	27	–	–	–
47963 <sup>2</sup>	989	15	1.5	1,261	17	1.3
GSE1-G	228	24	10.5	1,644	9	0.5
BHVO2-G	305	15	4.9	70	4	5.7
A500 <sup>3</sup>	–	–	–	690	5	0.7
RD5000 <sup>3</sup>	–	–	–	884	4	0.5

Glasses were analyzed with EPMA, and F and Cl concentrations were determined using our calibration lines (Figs. 1a–1c). Errors reported are  $2\sigma - \text{SE}$ . The glasses were synthesized by <sup>1</sup>Zhang et al. (2016), <sup>2</sup>Kendrick et al. (2012), and <sup>3</sup>Cadoux et al. (2017). Cl results are from Cadoux (personal communication).

## Analytical Methods

All samples were examined with a JEOL 6510LV scanning electron microscope (SEM), and the major element concentrations of all phases were determined with a 5-spectrometer JEOL JXA 8530F electron microprobe analyzer (EPMA) at the Institute für Mineralogie at the Westfälische Wilhelms-Universität Münster (WWU). Halogen-bearing silicate glasses were measured in a first step for concentrations of Na, Mg, Al, Si, K, Ca, Ti, Cr, Mn, and Fe. Conditions were 15 kV accelerating voltage, 5–15 nA beam current, and counting times of 10 s on the peak and 5 s on the background positions, except for Na and K (7 s on peak and 3 s on background). Spot size was varied of between 10 and 20  $\mu\text{m}$ . In a second step, halogens of the previously analyzed spots were measured with a beam current of 60 nA and

counting times of 120 s on the peak and 60 s on the background (Zhang et al., 2016). The individual sets of silicate and halogen analyses were eventually merged using the JEOL WDS software package to obtain full  $\varphi(\rho Z)$  matrix-corrected (Armstrong, 1984) quantitative analysis. Spectral overlaps of  $\text{FeL}_{\alpha}$  on  $\text{FK}_{\alpha}$ ,  $\text{AlK}_{\alpha}$  on  $\text{BrL}_{\beta}$ , and  $\text{CaK}_{\beta}$  on  $\text{IL}_{\alpha}$  were finally corrected using the previously determined correction factors. Details of EPMA halogen settings are summarized in Supplementary Table 1. Astimex Tugtupite, fluorite, and topaz were used as reference materials for F and Cl analyses, and Astimex TlBrI was used as a reference material for Br and I. Detection limits (DLs) are  $\sim 88 \mu\text{g/g}$  for F,  $\sim 28 \mu\text{g/g}$  for Cl,  $\sim 156 \mu\text{g/g}$  for Br, and  $\sim 76 \mu\text{g/g}$  for I, and were determined by the JEOL software using background statistics and the  $3\sigma$  criterion from equation 9.25 as described in Goldstein et al. (2018).

**Table 3.** Fluorine and Cl Contents of Reference Glasses from the Literature Compared With Our Study.

Glass	Analytical Method	F ( $\mu\text{g/g}$ )	Error	Cl ( $\mu\text{g/g}$ )	Error	F – accuracy (%)	Cl – accuracy (%)
VG-2 (Juan de Fuca) <sup>1</sup>	EPMA	–	–	316	19	–	13
VG-2 (Juan de Fuca) <sup>8</sup>	EPMA	–	–	329	5	–	16
VG-2 (Juan de Fuca) <sup>11</sup>	EPMA	301	19	303	20	44	9
VG-2 (Juan de Fuca) <sup>4</sup>	SIMS	334	14	–	–	49	–
VG-A99 (Makaopuhi) <sup>1</sup>	EPMA	–	–	227	20	–	7
VG-A99 (Makaopuhi) <sup>8</sup>	EPMA	–	–	271	9	–	23
VG-A99 (Makaopuhi) <sup>11</sup>	EPMA	874	98	225	14	33	7
VG-A99 (Makaopuhi) <sup>4</sup>	SIMS	709	47	–	–	17	–
VG-A99 (Makaopuhi) <sup>6</sup>	EPMA	976	4	–	–	40	–
VG-568 (Rhyolite) <sup>7</sup>	EPMA	–	–	1,013	53	–	0.2
VG-568 (Rhyolite) <sup>11</sup>	EPMA	1,968	56	1,045	35	9	3
BCR-2G <sup>11</sup>	EPMA	317	59	99	18	47	62
BCR-2G <sup>5</sup>	IC/ICP-MS	448	3	98	8	63	61
BCR-2G <sup>12</sup>	Noble gases	–	–	67	2	–	43
AC-E <sup>11</sup>	EPMA	1,890	64	292	17	0.3	4
AC-E <sup>5</sup>	IC/ICP-MS	1,807	184	162	91	4	87
AC-E <sup>10</sup>	IC/TXRF	1,962	93	261	22	4	16
GS-N <sup>11</sup>	EPMA	920	38	497	20	5	5
GS-N <sup>5</sup>	IC/ICP-MS	919	5	349	7	5	35
GS-N <sup>10</sup>	IC/TXRF	932	31	456	32	3	4
DR-N <sup>11</sup>	EPMA	573	71	521	23	2	9
DR-N <sup>10</sup>	IC/TXRF	567	97	545	25	3	13
DR-N <sup>13</sup>	EPMA	586	20	475	3	–	–
47963 <sup>9</sup>	Noble gases	–	–	1,356	–	–	7
47963 <sup>2,3</sup>	EPMA	780	–	1,400	–	27	10
GSE1-G <sup>12</sup>	EPMA/IC	150	15	1,300	75	52	26
BHVO2-G <sup>12</sup>	EPMA	305	20	80	15	0.1	13
BHVO2-G <sup>12</sup>	IC	295	25	70	15	3.5	0
A500 <sup>13</sup>	SIMS	–	–	603	7.5	–	14
RD5000 <sup>13</sup>	SIMS	–	–	762.5	12.1	–	15

<sup>1</sup>Thordarson et al. (1996); <sup>2</sup>Kamenetsky et al. (2000); <sup>3</sup>Kamenetsky & Maas (2002); <sup>4</sup>Straub & Layne (2003); <sup>5</sup>Michel & Villemant (2003); <sup>6</sup>Witter & Kuehner (2004); <sup>7</sup>Streck & Wacaster (2006); <sup>8</sup>van der Zwan et al. (2012); <sup>9</sup>Kendrick et al. (2012); <sup>10</sup>Wang et al. (2014); <sup>11</sup>Zhang et al. (2016); <sup>12</sup>Marks et al. (2016), Cadoux (personal communication). Errors reported are either SD,  $1\sigma$  or  $2\sigma$  depending on the study. The reported accuracy of our measurements is relative to the different methods (Column “Analytical Method”) used in different studies.

## Results and Discussion

### Calibration Lines

Electron microprobe analysis of F, Br, and I of geological samples is difficult due to interferences of Fe on F-lines, Al on Br-lines, and Ca on I-lines. Hence, we used Fe-, Al-, and Ca-bearing glasses to calibrate the aforementioned interferences. Here, it should be noted that the calibration lines (i.e., the measured Fe–F, Al–Br and Ca–Cl contents of the silicate glasses) can vary with beam current and other settings (e.g., baseline, window, bias, and gain). This indicates that the calibration lines (and equations) reported further below and in Figures 1a–1c will not be the same for other laboratories with a different instrument type and/or a different measurement setting. Thus, for other

instrument types and/or settings, new calibrations (following the same procedure) need to be performed, which are specifically designed for them. Moreover, to further assess the accuracy of the measurements, the calibrations for the measured elements should be periodically performed during each measurement session.

The calibration curves are depicted in Figures 1a–1c, and results are given in Tables 2 and 3. As an example, our analyses show a linear relationship between the “apparent” F signal and the Fe concentrations of the samples (Zhang et al., 2016), and the results may be described by the following linear equation:  $y = 65.209x + 287.93$  with  $R^2 = 0.9962$ . The  $2\sigma$  uncertainty on the “apparent” F content is  $\pm 40 \mu\text{g/g}$  but increases to  $\pm 80 \mu\text{g/g}$  for elevated Fe contents ( $>9 \text{ wt}\%$ ). We then use this calibration line (Fig. 1a) to correct our measured F concentrations in various

**Table 4.** Bromine Contents ( $\mu\text{g/g}$ ) and Accuracy of Reference Glasses Analyzed in Our Study and in Cadoux et al. (2017).

Glass	Analytical Method	Br	Error	Error %	Accuracy Br
GSE1-G	EPMA	423	27	6.4	–
A500 <sup>1</sup>	INAA	524	1.6	–	22
A500 <sup>1</sup>	LA-ICP-MS	423	11	–	3
A500 <sup>1</sup>	SIMS	381	20	–	7
A500 <sup>2</sup>	EPMA	409	15	3.7	–
A1000 <sup>1</sup>	INAA	990	3.2	–	3
A1000 <sup>1</sup>	LA-ICP-MS	1,102	192	–	7
A1000 <sup>1</sup>	SIMS	1,127	48	–	9
A1000 <sup>2</sup>	EPMA	1,024	26	2.5	–
RD5000 <sup>1</sup>	INAA	5,030	9	–	29
RD5000 <sup>1</sup>	LA-ICP-MS	5,355	635	–	22
RD5000 <sup>1</sup>	SIMS	5,638	310	–	16
RD5000 <sup>2</sup>	EPMA	6,522	67	1	–

Bromine concentrations were obtained using our calibration line. Errors reported from Cadoux et al. (2017) and the present study are  $2\sigma - \text{SE}$ . <sup>1</sup>Cadoux et al. (2017) and <sup>2</sup>present study. The reported accuracy of our measurements is relative to the different analytical methods (Column “Analytical Method”) used in different studies.

synthetic and natural halogen-bearing glasses from the literature, which have been used to check for the accuracy of halogen analyses in previous studies (Kamenetsky et al., 2000; Kamenetsky & Maas, 2002; Michel & Villemant, 2003; Straub & Layne, 2003; Kendrick et al., 2012; Marks et al., 2012, 2016; Wang et al., 2014; Zhang et al., 2016). Details of the glasses we analyzed [VG-2 (USNM 111240/52, basaltic glass), VG-A99 (USNM 113498/1, basaltic glass), VG-568 (USNM 7285, rhyolitic glass), NMNH 113716/11 (USNM, basaltic glass), BCR-2G (USGS,

basaltic glass), GSE1-G (USGS, basaltic glass), and BHVO2-G (USGS, basaltic glass)], the synthesized glasses from Zhang et al. (2016), AC-E (granite), GS-N (granite) and DR-N (diortite), and glass 47963 (basaltic glass) (Kamenetsky et al., 2000; Kamenetsky & Maas, 2002, in Kendrick et al., 2012) are presented in Tables 2 and 3. We then compared our results with literature values by Zhang et al. (2016), because we applied the same analytical rationale and one value from Marks et al. (2016) (Fig. 2a). The F precisions and accuracies of our analyses are given in Tables 2 and 3.

To account for the interference of Al- on Br-lines during EPMA analysis, we followed an identical approach (Fig. 1b). The “apparent” Br signal and the Al concentrations of the samples also follow a linear relationship, with  $y = 48.467x + 7.7809$  with an  $R^2 = 0.9891$ . At  $\text{Al}_2\text{O}_3$  contents  $< 12$  wt%,  $2\sigma$  uncertainty of the “apparent” Br of the sample increases from  $\sim 40$  to  $\sim 80$   $\mu\text{g/g}$ , mainly due to the lack of Br-free reference glasses with such low concentrations of  $\text{Al}_2\text{O}_3$ . We then used the new calibration line to analyze Br-bearing hydrous glasses from Cadoux et al. (2017), which were synthesized from natural volcanic rocks in various compositions (Table 2 and 3) and analyzed with *in situ* techniques such as SIMS, LA-ICP-MS, and synchrotron radiation X-ray fluorescence spectrometry (SR-XRF) (Cadoux et al., 2017). Our EPMA results agree well with the data from Cadoux et al. (2017) (Table 4).

We also prepared Ca-bearing I-free glasses which allowed us to quantify the effect of Ca in the signal of the I spectrum ( $\sim 20$ – $40$   $\mu\text{g/g}$ , Fig. 1c) during EPM analysis. Similar to F and Br, the “apparent” I signal shows a linear relationship with the Ca concentration of the samples, with  $y = 43.179x + 37.555$  with an  $R^2 = 0.9958$ . As there are no available reference glasses for I analyses, we could not apply our new method to the aforementioned glasses.

The analysis of Cl with EPMA, however, does not require correction. We, therefore, measured the Cl content of the same synthetic and natural halogen-bearing glasses (Table 2) and then compared our results with the literature (Kamenetsky et al., 2000; Kamenetsky & Maas, 2002; Michel & Villemant, 2003; Straub & Layne, 2003; Kendrick et al., 2012; Marks et al., 2012,

**Table 5.** Major Elements (wt%) and Halogen Concentrations ( $\mu\text{g/g}$ ) of Experimental Glasses.

Glass	SF-G8	SF-G9
$\text{SiO}_2$	50.8	51.4
$\text{Al}_2\text{O}_3$	12.7	13.1
FeO	0.5	0.1
MgO	8.2	8.6
CaO	20.4	20.7
$\text{Na}_2\text{O}$	3.1	2.4
$\text{K}_2\text{O}$	1.5	1.2
F	3,592	516
Error (SD)	65	43
Cl	5,098	1189
Error (SD)	26	17
Br	3,674	709
Error (SD)	63	42
I	5,471	981
Error (SD)	62	44

Halogen-bearing synthetic experimental glasses are SF-G8 and -G9 (this study). The nominal starting material compositions for each halogen were 5,000  $\mu\text{g/g}$  for SF-G8 and 1,000  $\mu\text{g/g}$  for SF-G9.



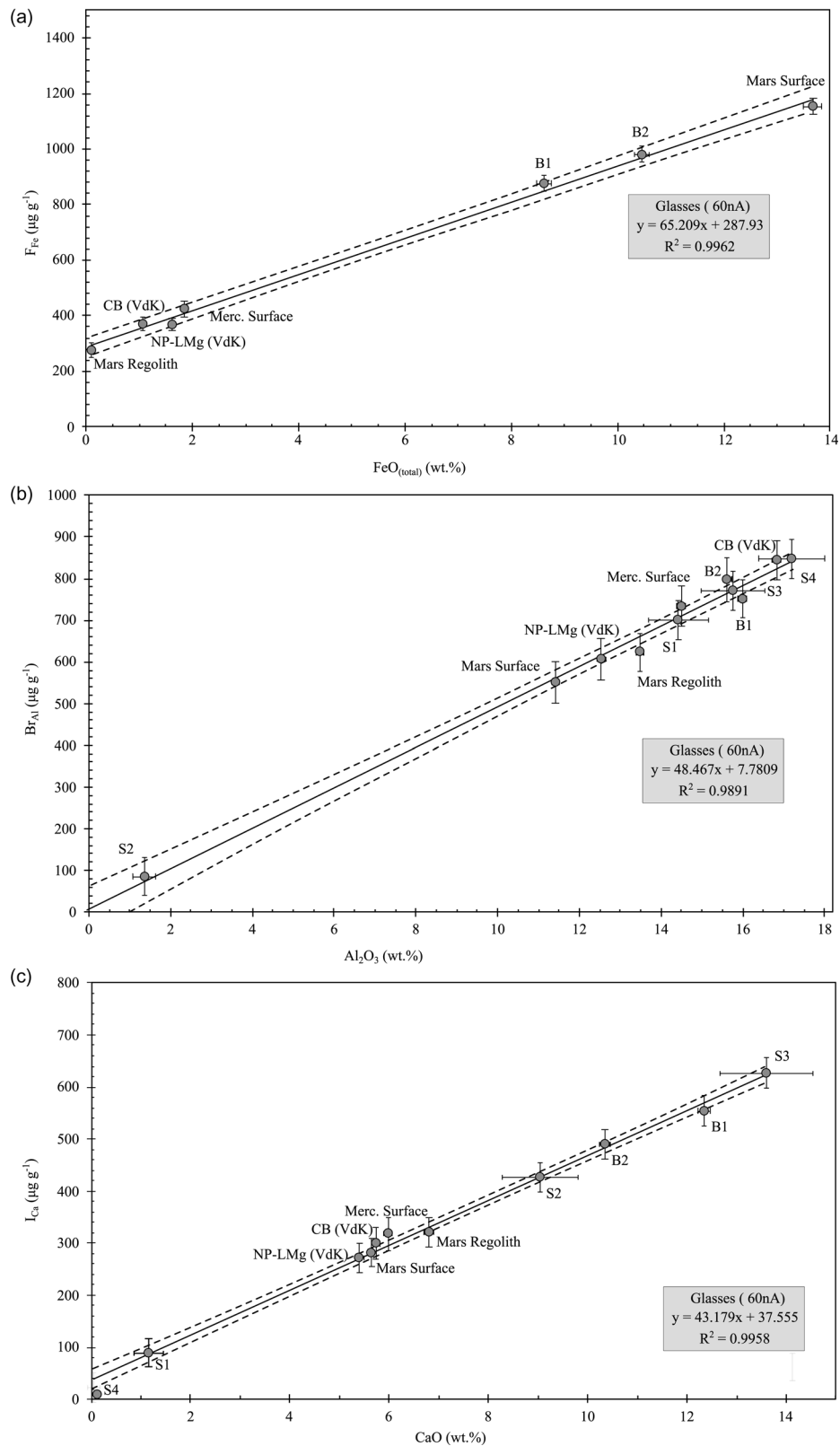


**Fig. 1.** (a) Calibration line for F. Glasses with different Fe contents were used from ~0.4 to ~14 wt% (Table 1). There is an almost linear correlation ( $R^2 = 0.9962$ ) with increasing Fe content. The 95.45% confidence line indicates that the error (2 SD) on the F content because of Fe is relatively small ( $\pm 40 \mu\text{g/g}$ ) up to ~9 wt% and increases ( $\pm 80 \mu\text{g/g}$ ) at higher concentrations. (b) Calibration line for Br that quantifies the effect of Al in the analysis signal. Our glasses have an  $\text{Al}_2\text{O}_3$  content ranging from ~1 to ~18 wt% (Table 1). The excess Br signal we get from Al also shows a linear relation ( $R^2 = 0.9891$ ) with an increasing amount of Al inside the samples. Based on the 95.45% confidence lines, the error (2 SD) at the excess Br for Al concentrations higher than 12 wt% is  $\pm 20 \mu\text{g/g}$ , while it increases significantly at concentrations less than 2 wt%, probably due to the absence of glasses with very low Al contents. (c) Calibration line for I shows the effect of Ca-interference on the I measurements. The Ca compositional range of our glasses is from 0.4 to ~14 wt% (Table 1). The correlation between the glasses with different Ca contents and the excess I in the signal of the analysis has a linear correlation ( $R^2 = 0.9958$ ). The 95% confidence lines show that the error (2 SD) at the excess I for Ca concentrations from ~5 to ~14 wt% is  $\pm 20 \mu\text{g/g}$ , while it increases at low concentrations (<2 wt%) at  $40 \mu\text{g/g}$ .

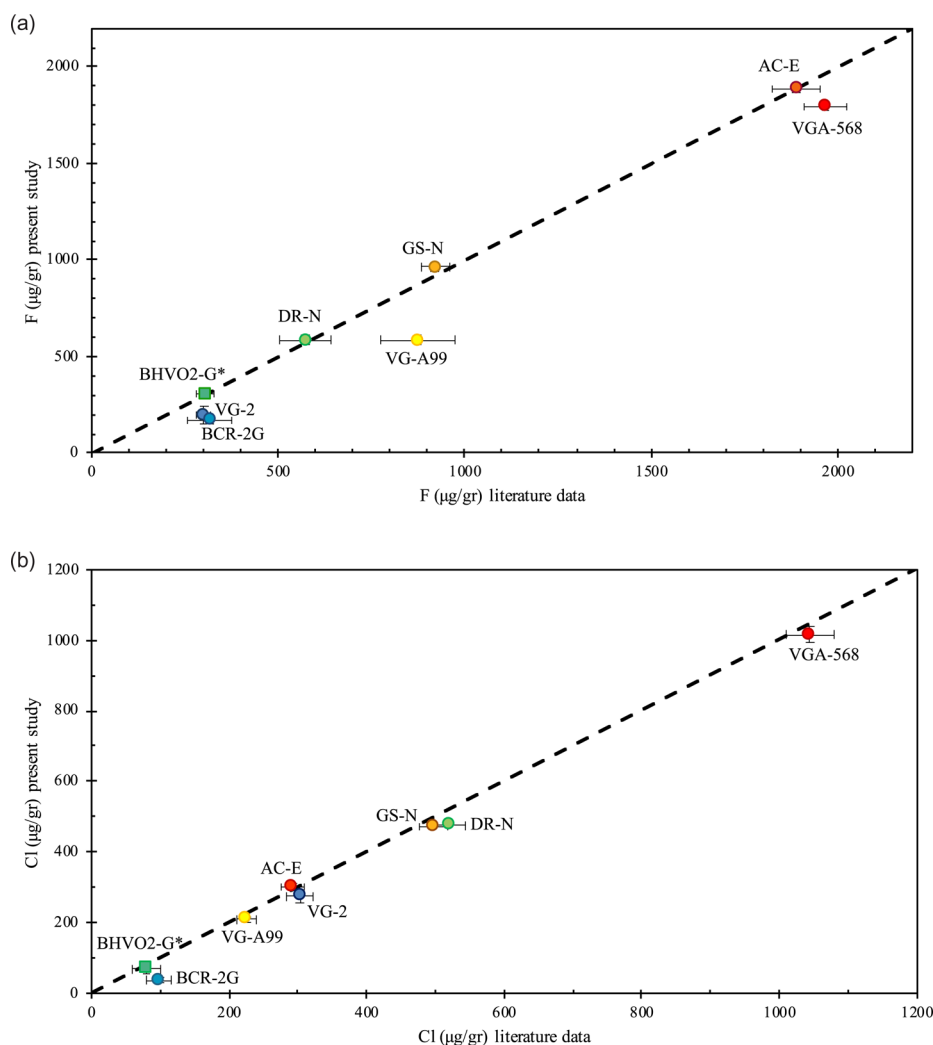


**Fig. 2.** (a) Fluorine literature data for the glasses VG-A99, VGA-568, VG-2, AC-E, DR-N, GS-N, BCR-2G, and BHVO2-G (Marks et al., 2016; Zhang et al., 2016), compared with F data from the present study. Fluorine concentrations from each study can be found in Tables 2 and 3. The dashed line represents the 1:1 line. Our results are plotted mainly against the data from Zhang et al. (2016), in order to show the good agreement of the individual studies. Glasses VGA-568, VG-A99, and VG-2 show differences that are discussed inside the text and are attributed to glass inhomogeneity. (b) Chlorine literature data for the glasses VG-A99, VGA-568, VG-2, AC-E, DR-N, GS-N, BCR-2G, and BHVO2-G (Marks et al., 2016; Zhang et al., 2016), compared with Cl data from the present study. Chlorine concentrations from each study can be found in Tables 2 and 3. The dashed line represents the 1:1 line. Our results are plotted mainly against the data from Zhang et al. (2016) and show an overall excellent agreement.

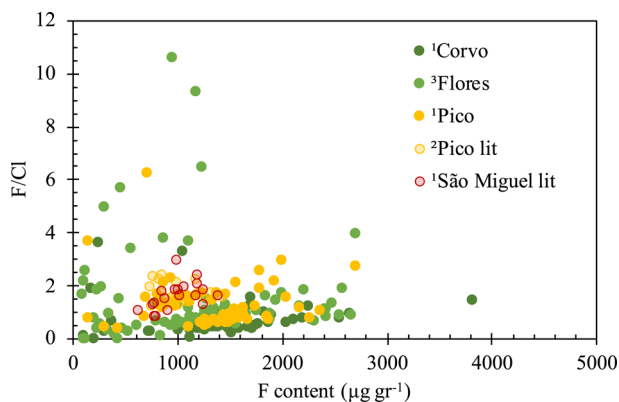


**Fig. 3.** Fluorine versus Cl data in olivine-hosted melt inclusions from the Azores show good agreement between datasets obtained with different instruments and methods. Particularly, the two datasets obtained on melt inclusions from Pico island span the same Cl-F space. <sup>1</sup>Present study, <sup>2</sup>Métrich et al. (2014), and <sup>3</sup>Rose-Koga et al. (2017). The table with the individual data can be found in Supplementary Table 2.

2016; Wang et al., 2014; Zhang et al., 2016). Chlorine contents of analyzed glasses along with the accuracy (relative to other studies) and precision of our measurements are summarized in Tables 2 and 3. We also compared our data with the results from Zhang et al. (2016), and one value from Marks et al. (2016) (Fig. 2b).

### Fluorine

Fluorine precision of the analyzed glasses (Table 2) ranges between ~1 and 27%. Glasses GSE1-G ( $228 \pm 24 \mu\text{g/g}$ ), BCR2-G ( $167 \pm 19 \mu\text{g/g}$ ), VG-2 ( $197 \pm 46 \mu\text{g/g}$ ), and NMNH 113716/11 ( $153 \pm 41 \mu\text{g/g}$ ) show a precision that varies from 10.5 to 27%. For the rest of the glasses, i.e., VG-568 ( $1,794 \pm 21 \mu\text{g/g}$ ), 47963 ( $989 \pm 15 \mu\text{g/g}$ ), VGA-99 ( $585 \pm 26 \mu\text{g/g}$ ), AC-E ( $1,885 \pm 20 \mu\text{g/g}$ ), GS-N ( $963 \pm 22 \mu\text{g/g}$ ), DR-N ( $586 \pm 20 \mu\text{g/g}$ ), BHVO2-G ( $305 \pm 15 \mu\text{g/g}$ ), precision ranges from 1 to 4.9% (Table 2).

The accuracy of the F analyses between individual studies and the present study varies from <1 to up to 63% and seems

independent of absolute F contents. Our results for the glasses, VG-568, AC-E, GS-N, DR-N, BVO2-G, and 47963, agree with published literature values with an accuracy ranging from <0.2 to 9% (Table 3), especially with the results from Zhang et al. (2016) (Fig. 2a). Reference glasses VG-A99, VG-2, BCR2-G, and GSE1-G show the lowest accuracy between the individual studies (Table 3). In VG-A99, our results, compared with the studies of Zhang et al. (2016), Witter & Kuehner (2004), and Straub & Layne (2003), show an accuracy that ranges between 17 and 40%. For BCR-2G, compared with Michel & Villemant (2003) and Zhang et al. (2016), the accuracy is 63 and 47% respectively. For VG-2, the accuracy is 44 and 49%, compared with Zhang et al. (2016) and Straub & Layne (2003), respectively. Marks et al. (2016) is the only study that reported values for GSE1-G, and in this case, the accuracy is 52%. All the F contents, errors, accuracy, and analytical methods used, for each study, can be found in Table 3.

In summary, we find overall good agreement of our EPMA data with analytical results of previous studies, and this provides a strong support for the validity of our new analytical method. Note that our EPMA data for some glasses differ from the literature results in terms of F (Table 3, glasses VG-A99, VG2, BCR2-G, and GSE-1G). The reasons for this are unclear, but this may be due to heterogeneity of F in the samples. Therefore, we conclude that glasses VG-568, AC-E, GS-N, DR-N, BVO2-G, and 47963 are suitable as reference materials for EPMA analysis, while we would caution the reader to use VG-A99, VG-2, BCR-2G, and GSE-1G as reference materials for the micro-analysis of F. Here, it must be noted that accuracy is how well the values match with the “true” concentration of an element, in this case F. But the literature values are far from being true as there are either not enough data available to give a “compiled” true value, or, where enough data exist, they show a great dispersion. So, the accuracy that we present here is not the accuracy of the reference glasses, as their “true” values are not known; instead, we show the accuracy of our results with individual studies. Where F from individual studies agree well, then these glasses are recommended as an appropriate reference material for F analyses.

### Chlorine

Chlorine precision of the analyzed glasses (Table 2) ranges from 0.5 to 6.5%, with only glass BCR-2G showing a somewhat lower precision (23.5%), but with concentrations very close to the detection limit (i.e., 38  $\mu\text{g/g}$ ). For glasses GSE1-G (1,644  $\pm$  9  $\mu\text{g/g}$ ), VG-2 (275  $\pm$  18  $\mu\text{g/g}$ ), VG-568 (1,015  $\pm$  24  $\mu\text{g/g}$ ), 47963 (1,261  $\pm$  17  $\mu\text{g/g}$ ), VGA-99 (210  $\pm$  7  $\mu\text{g/g}$ ), AC-E (303  $\pm$  7  $\mu\text{g/g}$ ), GS-N (472  $\pm$  4  $\mu\text{g/g}$ ), DR-N (475  $\pm$  3  $\mu\text{g/g}$ ), and BHVO2-G (70  $\pm$  4  $\mu\text{g/g}$ ), precision ranges from 0.5 to 6.5%. Glasses A500 (690  $\pm$  5  $\mu\text{g/g}$ ) and RD5000 (880  $\pm$  4  $\mu\text{g/g}$ ), from Cadoux et al. (2017), showed a precision of 0.7 and 0.5%.

In regard to Cl (Table 3), the accuracy of our results ranges from <1% to up to 87% (Table 3) and looks independent of Cl concentrations. Overall, the accuracy, especially between our study and Zhang et al. (2016), is very good (0.2–9%) as can be seen in Table 3 and Figure 2b. Concerning glasses A500 and RD5000 from Cadoux et al. (2017), Cadoux (personal communication, 2020) determined the Cl content of the glasses by SIMS at 603  $\pm$  7.5  $\mu\text{g/g}$  and 762.5  $\pm$  12.1 (errors are 2 $\sigma$  – SE), which is an accuracy of 14 and 15%, respectively. The highest deviation of our results between published values is observed between our results and the data from Michel & Villemant (2003), for the

glasses BCR-2G, GS-N, and AC-E (62, 35, and 87%, respectively). Michel & Villemant (2003) used bulk methods such as pyrohydrolysis, ion chromatography, and ICP-MS to determine the Cl content of the glasses. As our EPMA data are substantially higher than the results from the bulk methods, we surmise that the glasses are heterogeneous, and that our small glass chips contain higher Cl concentrations than the bulk. We would, therefore, like to caution the reader when using these glasses as reference materials for Cl analyses of geological samples.

### Bromine

As to Br, our DLs are somewhat improved,  $\sim$ 156  $\mu\text{g/g}$ , compared with Zhang et al. (2017), 120–300  $\mu\text{g/g}$ . At the present, we cannot compare our results with natural glass reference materials, as these glasses contain only very small amounts of Br (usually less than 1 ppm), which is below the limit of detection for our EPMA method (Bureau et al., 2000; Kutterolf et al., 2013; Kendrick et al., 2014; Bureau, 2018). However, when we compare our EPMA results with synthetic Br-bearing glasses Cadoux et al. (2017), we find that our method can reproduce the literature values with good accuracy (Table 4). We re-analyzed glasses A500, A1000, and RD5000 (Cadoux et al., 2017). For A500, we obtain a Br content of 409  $\pm$  42  $\mu\text{g/g}$  (precision 3.8%), that is lower to the INAA reference value (524  $\pm$  1.6  $\mu\text{g/g}$ ) and similar to those measured by LA-ICP-MS and SIMS (423  $\pm$  11  $\mu\text{g/g}$ , accuracy 3%; and 381  $\pm$  20  $\mu\text{g/g}$ , accuracy 7%, respectively; Cadoux et al., 2017). Glass A1000 yielded a Br content of 1,030  $\pm$  163  $\mu\text{g/g}$  (precision 2.5%), which is consistent with the INAA reference value of 990  $\pm$  3.2  $\mu\text{g/g}$  (accuracy 3%) and similar to the contents measured by LA-ICP-MS and SIMS (1,102  $\pm$  192  $\mu\text{g/g}$ , accuracy 7%; and 1,127  $\pm$  48  $\mu\text{g/g}$ , accuracy 9%, respectively; Cadoux et al., 2017). Finally, for RD5000, we obtain a Br content of 6,512  $\pm$  204  $\mu\text{g/g}$  (precision 1.0%), which is higher than the INAA values of 5,030  $\pm$  9 but close to the contents, within error, obtained by other *in situ* analyses: 5,355  $\pm$  635  $\mu\text{g/g}$  (accuracy 22%) with LA-ICP-MS and 5,638  $\pm$  310  $\mu\text{g/g}$  (accuracy 16%) with SIMS (Cadoux et al., 2017).

### Iodine

We also present a novel analytical protocol for I analyses with EPMA, with DLs between  $\sim$ 76 and  $\sim$ 150  $\mu\text{g/g}$  I. Although this detection limit is probably too high for I concentrations in natural glasses (Bureau et al., 2000, 2016; Kendrick et al., 2014; Bureau, 2018), we can use our EPMA method to analyze experimental samples that have been doped with I. These experiments could be interesting to study I speciation in glasses, or investigate I solubility in silicate melts, or the I partitioning between crystals and melts or between immiscible melts (Steenstra et al., 2020).

### New Experimental Halogen-Bearing Glasses

The good agreement of our F, Cl, and Br EPMA measurements with those of previous studies provides strong support in the use of our calibration lines to quantify halogen contents in silicate glasses.

To extend the applicability of our method, we additionally analyzed the two synthetic basaltic glasses doped with different amounts of F, Br, and I: glass SFG8 (5,000  $\mu\text{g/g}$  for each halogen) and glass SFG9 (1,000  $\mu\text{g/g}$  for each halogen). The calibration lines were used to subtract the “apparent” halogen contents.



Sixty separate analyses were performed on each glass. The results are reported in Table 5, and the uncertainty associated with each value represents the  $2\sigma$  – SE. Glass SFG8 has an F content of  $3,592 \pm 24 \mu\text{g/g}$  (precision 0.7%), Cl content of  $5,098 \pm 10 \mu\text{g/g}$  (precision 0.2%), Br content of  $3,674 \pm 23 \mu\text{g/g}$  (precision 0.6%), and I content of  $5,482 \pm 24 \mu\text{g/g}$  (precision 0.4%). Glass SFG9 has an F content of  $529 \pm 11 \mu\text{g/g}$  (precision 2.2%), Cl content of  $1,187 \pm 4 \mu\text{g/g}$  (precision 0.4%), Br content of  $713 \pm 11 \mu\text{g/g}$  (precision 1.6%), and I content of  $996 \pm 12 \mu\text{g/g}$  (precision 1.2%). The accuracy of our glasses can be compared only with the amount that we weighted inside. We see that our assumed values agree almost perfectly for Cl and I for all glasses (weighted amounts 5,000 and 1,000  $\mu\text{g/g}$ , with accuracies of 2 and 19% for Cl, respectively; 10 and 0% for I) but not for F and Br, and that assumed values have an accuracy of 28 and 47% for F, respectively; 27 and 29%, for Br, respectively.

Concerning the in-house halogen-bearing glasses that we prepared (SFG-8 and -9), since the accuracy for Cl and I, in individual samples, is the same (Table 5), and the relative accuracy for Br and F is the same (Table 5), we can assume that the difference between the amount of halogens put in the starting mixture and the analyzed amount in the experimental samples is attributed to impurities and inhomogeneity of the chemical compounds used. In principle, no special treatment is needed for obtaining Cl contents; hence, we used the Cl concentrations to rule out potential loss of other halogens during preparation of the experimental glasses. Thus, we are confident that, by using our calibration lines, we accurately determined the F, Br, and I contents of the glasses. Moreover, the overall good precision and accuracy of our results for reference materials suggest that our in-house glasses are homogeneous and accurate. However, future studies should confirm the accuracy of our analyses with alternative analytical methods.

### Analyses of Glasses in Natural Melt Inclusions

A promising application of our EPMA method lies in the analysis of the halogen contents of natural melt inclusions. To show some examples of how our method could be used, we analyzed all four halogens in olivine-hosted melt inclusions from Corvo and Pico Island in the Azores. F and Cl abundances in melt inclusions from the Pico were previously determined by EPMA by Métrich et al. (2014). All analytical results are given in Supplementary Table 2. We compare our data with the Métrich results in Figure 3, and we find very good agreement between the two datasets for both F and Cl. Furthermore, the melt inclusion data from São Miguel (eastern Azores, Rose-Koga et al., 2017, obtained by SIMS) and from Corvo (western Azores, this study) reveal compositional differences between different islands, but the reader is referred to the studies of Métrich et al. (2014) and Rose-Koga et al. (2017) for further discussion on these matters.

### Conclusions

- We produced four synthetic silicate glasses without halogens. These glasses were used to account and correct for the spectral interferences of Fe on F, Al on Br, and Ca on I peaks.
- We present a robust (high accuracy, high precision, and with improved DLs) electron microprobe method that enables the simultaneous determination of F, Br, Cl, and I contents in silicate glasses.

- We also present a novel analytical protocol for the analysis of I with EPMA in silicate glasses.
- Applying this new EPMA method, we analyzed several international reference glasses. The results show that some glasses (VG-A99, VG-2, and BCR-2G) are heterogeneous with respect to halogens and should not be used. However, other reference materials, such as VG-568, AC-E, GS-N, DR-N, and 4796, are much better suited and can be recommended for future halogen studies.
- Potential applications of this readily accessible method are demonstrated for the routine halogen analyses of experimental samples, melt inclusions, and natural glasses in a wide compositional spectrum (100's of  $\mu\text{g/g}$  to 1,000's of  $\mu\text{g/g}$ ).
- Further improvements of the analytical precision will require sets of reference glasses with lower concentrations especially at the tens of  $\mu\text{g/g}$  to sub- $\mu\text{g/g}$  level, which is the range of Br and I contents in most natural glasses.

**Supplementary material.** To view supplementary material for this article, please visit <https://doi.org/10.1017/S1431927620013495>.

**Acknowledgments.** We thank Beate Schmitte and Maik Trogisch for sample preparation and support during the electron microprobe measurements. Moreover, we also thank the members of the workshops at the Institute for Mineralogy (M. Feldhaus, J. Kemmann, P. Weitkamp, H. Heying, L. Buxtrup, and A. Gerdes) for their sterling efforts in the labs. This work was supported by the DFG (SFB-TRR 170, publ. no. 105).

### References

- Armstrong JT (1984). Quantitative analysis of silicate and oxide minerals: A reevaluation of ZAF corrections and proposal for new Bence-Albee coefficients. *Microbeam Analysis* **19**, 208–212.
- Bénard A, Koga KT, Shimizu N, Kendrick MA, Ionov DA, Nebel O & Arculus RJ (2017). Chlorine and fluorine partition coefficients and abundances in sub-arc mantle xenoliths (Kamchatka, Russia): Implications for melt generation and volatile recycling processes in subduction zones. *Geochimica et Cosmochimica Acta*. **199**.324–350.<http://dx.doi.org/10.1016/j.gca.2016.10.035>.
- Berndt J, Koepke J & Holtz F (2005). An experimental investigation of the influence of water and oxygen fugacity on differentiation of MORB at 200 MPa. *J Petrol* **46**, 135–167.
- Bureau H (2018). Iodine. In *Encyclopedia of Geochemistry: A Comprehensive Reference Source on the Chemistry of the Earth*, White WM (Ed.), pp. 728–731. Springer International Publishing.
- Bureau H (2018). Bromine. In *Encyclopedia of Geochemistry: A Comprehensive Reference Source on the Chemistry of the Earth*, White WM (Ed.), pp. 167–170. Springer International Publishing.
- Bureau H, Auzende A-L, Marocchi M, Raepsaet C, Munsch P, Testemale D, Mézouar M, Kubsy S, Carrière M, Ricolleau A & Fiquet G (2016). Modern and past volcanic degassing of iodine. *Geochim Cosmochim Acta* **173**, 114–125.
- Bureau H, Keppler H & Métrich N (2000). Volcanic degassing of bromine and iodine: experimental fluid/melt partitioning data and applications to stratosphere chemistry. *Earth Planet Sci Lett* **183**, 51–60.
- Bureau H & Métrich N (2003). An experimental study of bromine behaviour in water-saturated silicic melts. *Geochimica et Cosmochimica Acta*. **67**(9), 1689–1697.
- Cadoux A, Iacono-Marziano G, Paonita A, Deloule E, Aiuppa A, Nelson Eby G, Costa M, Brusca L, Berlo K, Geraki K, Mather TA, Pyle DM & Di Carlo I (2017). A new set of standards for in situ measurement of bromine abundances in natural silicate glasses: Application to SR-XRF, LA-ICP-MS and SIMS techniques. *Chem Geol* **452**, 60–70.
- Fleet ME (1989). Structures of Sodium Alumino-Germanate Sodalites  $[\text{Na}_8(\text{Al}_6\text{Ge}_6\text{O}_{24})\text{A}_2, \text{A} = \text{Cl}, \text{Br}, \text{I}]$ . *Acta Crystallographica Section C*. **45**.843–847.

- Goldstein J, Newbury DE, Michael JR, Ritchie NWM, Scott JHJ & Joy DC (2018). *Scanning Electron Microscopy and X-Ray Microanalysis*, 4th ed. New York, NY: Springer.
- Hammerli J, Rusk B, Spandler C, Emsbo P & Oliver NHS (2013). In situ quantification of Br and Cl in minerals and fluid inclusions by LA-ICP-MS: A powerful tool to identify fluid sources. *Chem Geol* **337–338**, 75–87.
- Harlov DE & Aranovich L (Eds.) (2018). *The Role of Halogens in Terrestrial and Extraterrestrial Geochemical Processes*. Cham: Springer International Publishing. Available at <http://link.springer.com/10.1007/978-3-319-61667-4>
- Hinton RW (1990). Ion microprobe trace-element analysis of silicates: Measurement of multi-element glasses. *Chem Geol* **83**, 11–25.
- Jarosewich E, Nelen JA & Norberg Julie A. (1980). Reference Samples for Electron Microprobe Analysis\*. *Geostandards and Geoanalytical Research* **4**(1), 43–47. doi: <http://dx.doi.org/10.1111/ggr.1980.4.issue-1>.
- Kamenetsky VS, Everard JL, Crawford AJ, Varne R, Eggins SM & Lanyon R (2000). Enriched end-member of primitive MORB melts: Petrology and geochemistry of glasses from Macquarie Island (SW Pacific). *J Petrol* **41**, 411–430.
- Kamenetsky VS & Maas R (2002). Mantle-melt evolution (dynamic source) in the origin of a single MORB suite: A perspective from Magnesian glasses of Macquarie Island. *J Petrol* **43**, 1909–1922.
- Kendrick MA (2012). High precision Cl, Br and I determinations in mineral standards using the noble gas method. *Chem Geol* **292–293**, 116–126.
- Kendrick MA, Arculus RJ, Danyushevsky LV, Kamenetsky VS, Woodhead JD & Honda M (2014). Subduction-related halogens (Cl, Br and I) and H<sub>2</sub>O in magmatic glasses from Southwest Pacific Backarc Basins. *Earth Planet Sci Lett* **400**, 165–176.
- Kendrick MA, Honda M, Pettke T, Scambelluri M, Phillips D & Giuliani A (2013). Subduction zone fluxes of halogens and noble gases in seafloor and forearc serpentinites. *Earth and Planetary Science Letters* **365**:86–96.
- Kendrick MA, Jackson MG, Hauri EH & Phillips D (2015). The halogen (F, Cl, Br, I) and H<sub>2</sub>O systematics of Samoan lavas: Assimilated-seawater, EM2 and high-<sup>3</sup>He/<sup>4</sup>He components. *Earth and Planetary Science Letters* **410**:197–209.
- Kendrick MA, Kamenetsky VS, Phillips D & Honda M (2012). Halogen systematics (Cl, Br, I) in mid-ocean ridge basalts: A Macquarie Island case study. *Geochim Cosmochim Acta* **81**, 82–93.
- Klemme S & Stalder R (2018). Halogens in the Earth's mantle: What we know and what we don't. In *The Role of Halogens in Terrestrial and Extraterrestrial Geochemical Processes: Surface, Crust, and Mantle*, Harlov DE & Aranovich L (Eds.), pp. 847–869. Cham: Springer International Publishing. doi:10.1007/978-3-319-61667-4\_14.
- Kusebauch C, John T, Whitehouse MJ, Klemme S & Putnis A (2015). Distribution of halogens between fluid and apatite during fluid-mediated replacement processes. *Geochimica et Cosmochimica Acta* **170**:225–246. <http://dx.doi.org/10.1016/j.gca.2015.08.023>.
- Kutterolf S, Hansteen TH, Appel K, Freundt A, Krüger K, Pérez W & Wehrmann H (2013). Combined bromine and chlorine release from large explosive volcanic eruptions: A threat to stratospheric ozone? *Geology* **41**, 707–710.
- Lerouge C, Claret F, Denecke MA, Wille G, Falkenberg G, Ramboz C, Beny C, Giffaut E, Schäfer T, Gaucher EC & Tournassat C (2010). Comparative EPMA and  $\mu$ -XRF methods for mapping micro-scale distribution of iodine in biocarbonates of the Callovian–Oxfordian clayey formation at Bure, Eastern part of the Paris Basin. *Phys Chem Earth Parts A/B/C* **35**, 271–277.
- Louvel M, Sanchez-Valle C, Malfait WJ, Pokrovski GS, Borca CN & Grolimund D (2020). Bromine speciation and partitioning in slab-derived fluids and melts: Implications for halogens recycling in subduction zones. *Solid Earth Sci.* **11**, 1145–1147.
- Marks MAW, Kendrick MA, Eby GN, Zack T & Wenzel T (2016). The F, Cl, Br and I contents of reference glasses BHVO-2G, BIR-1G, BCR-2G, GSD-1G, GSE-1G, NIST SRM 610 and NIST SRM 612. *Geostand Geoanal Res* **41**, 107–122.
- Marks MAW, Wenzel T, Whitehouse MJ, Loose M, Zack T, Barth M, Worgard L, Krasz V, Eby GN, Stosnach H & Markl G (2012). The volatile inventory (F, Cl, Br, S, C) of magmatic apatite: An integrated analytical approach. *Chemical Geology* **291**, 241–255. doi:10.1016/j.chemgeo.2011.10.026.
- Métrich N, Zanon V, Créon L, Hildenbrand A, Moreira M & Marques FO (2014). Is the 'Azores Hotspot' a Wetspot? Insights from the geochemistry of fluid and melt inclusions in olivine of pico basalts. *J Petrol* **55**, 377–393.
- Michel A & Villemant B (2003). Determination of halogens (F, Cl, Br, I), sulfur and water in seventeen geological reference materials. *Geostand Geoanal Res* **27**, 163–171.
- Morlok A, Klemme S, Weber I, Stojic A, Sohn M & Hiesinger H (2017). IR spectroscopy of synthetic glasses with mercury surface composition: Analogs for remote sensing. *Icarus* **296**, 123–138.
- Morlok A, Klemme S, Weber I, Stojic A, Sohn M, Hiesinger H & Helbert J (2019). Mid-infrared spectroscopy of planetary analogs: A database for planetary remote sensing. *Icarus* **324**, 86–103.
- Pan Y & Dong P (2003). Bromine in Scapolite-group minerals and Sodalite: XRF Microprobe analysis, exchange experiments, and application to skarn deposits. *The Canadian Mineralogist* **41**:529–540.
- Potts PJ & Tindle AG (1989). Analytical characteristics of a multilayer dispersion element ( $2d = 60 \text{ \AA}$ ) in the determination of fluorine in minerals by electron microprobe. *Mineralogical Magazine* **53**:357–362.
- Rose-Koga EF, Koga KT, Moreira M, Vlastelic I, Jackson MG, Whitehouse MJ, Shimizu N & Habib N (2017). Geochemical systematics of Pb isotopes, fluorine, and sulfur in melt inclusions from São Miguel, Azores. *Chem Geol* **458**, 1–46.
- Steenstra E, van Haaster F, van Mulligen R, Flemetakis S, Berndt J, Klemme S & van Westrenen W (2020). An experimental assessment of the chalcophile behavior of F, Cl, Br and I: Implications for the fate of halogens during planetary accretion and the formation of magmatic ore deposits. *Geochimica et Cosmochimica Acta* **273**:275–290. doi:10.1016/j.gca.2020.01.006.
- Straub SM & Layne GD (2003). The systematics of chlorine, fluorine, and water in Izu arc front volcanic rocks: Implications for volatile recycling in subduction zones. *Geochim Cosmochim Acta* **67**, 4179–4203.
- Streck MJ & Wacaster S (2006). Plagioclase and pyroxene hosted melt inclusions in basaltic andesites of the current eruption of Arenal volcano, Costa Rica. *J Volcanol Geotherm Res* **157**, 236–253.
- Thordarson T, Self S, Óskarsson N & Hulsebosch T (1996). Sulfur, chlorine, and fluorine degassing and atmospheric loading by the 1783–1784 AD Laki (Skaftár Fires) eruption in Iceland. *Bull Volcanol* **58**, 205–225.
- van der Zwan FM, Fietzke J & Devey CW (2012). Precise measurement of low (<100 ppm) chlorine concentrations in submarine basaltic glass by electron microprobe. *J Anal Atom Spectrom* **27**, 1966.
- Wang L-X, Marks MAW, Keller J & Markl G (2014). Halogen variations in alkaline rocks from the Upper Rhine Graben (SW Germany): Insights into F, Cl and Br behavior during magmatic processes. *Chem Geol* **380**, 133–144.
- Witter JB & Kuehner SM (2004). A simple empirical method for high-quality electron microprobe analysis of fluorine at trace levels in Fe-bearing minerals and glasses. *Am Mineral* **89**, 1–7.
- Zhang C, Koepke J, Wang L-X, Wolff PE, Wilke S, Stechern A, Almeev RR & Holtz F (2016). A practical method for accurate measurement of trace level fluorine in Mg- and Fe-bearing minerals and glasses using electron probe microanalysis. *Geostand Geoanal Res* **40**, 351–363.
- Zhang C, Lin J, Pan Y, Feng R, Almeev RR & Holtz F (2017). Electron probe microanalysis of bromine in minerals and glasses with correction for spectral interference from aluminium, and comparison with microbeam synchrotron X-ray fluorescence spectrometry. *Geostand Geoanal Res* **41**, 449–457.